21 CM OBSERVATIONS OF NGC 300

By R. R. Shobbrook* and B. J. Robinson†

[*Manuscript received October* 3, 1966]

Summary

The 210 ft radio telescope at Parkes has been used to determine the profiles of the 21 cm line from neutral hydrogen at about 100 points over the Sc galaxy NGC 300. The systemic velocity is $+145$ km/sec, and the mass of neutral hydrogen is $2\cdot1\times10^{9}$ $M_{\odot}$. The total mass, determined from a rotation curve constructed from the velocities of the peaks of the profiles, is $2\cdot5\times10^{10}$ $M_{\odot}$, for an assumed distance of $1\cdot9$ Mpc.

There is a large cloud of neutral hydrogen, extending over at least $4°\cdot5$ by $3°$, situated to the south-east of NGC 300. This cloud has a velocity with respect to the Sun of $+40$ km/sec. In view of the fact that the velocity contours and the neutral hydrogen contours in the galaxy are quite strongly distorted in the direction of this cloud, it is suspected that the cloud lies near NGC 300. It then has a neutral hydrogen mass of the order of 10^{8}–10^{9} $M_{\odot}$.

I. Introduction

This paper is the third in a series of reports on observations of the 21 cm line from neutral hydrogen in external galaxies. The observations were made using the 210 ft radio telescope at Parkes, N.S.W., with a frequency-switching parametric receiver (Robinson and van Damme 1966).

Line profiles have been determined for a grid of over 100 points across the Sc galaxy NGC 300, plus about 20 points in a large adjacent HI region.

From the velocities of the peaks of these profiles a rotation curve for the galaxy has been constructed and the total mass and mass distribution determined. The areas under the profiles are used to find the mass of neutral hydrogen in NGC 300 and to estimate that of the neighbouring HI cloud. For the latter we have to assume a distance in order to determine a mass, and evidence for its being situated at the same distance as NGC 300 is discussed.

II. Observations

The half-power beamwidth of the Parkes paraboloid is $13'\cdot5$ at a wavelength of 21 cm. The telescope was equipped for these observations with a frequency-switching parametric receiver having a half-power bandwidth of 140 kHz, equivalent to 30 km/sec in radial velocity. The receiver sensitivity was calibrated frequently by injecting noise at the input from an argon discharge tube modulated in synchronism with the phase sensitive detector. This noise source was calibrated by comparison with the continuum source 3C 353 in order to establish an absolute scale of flux. The methods employed for the measurements of the constants of the receiver and telescope are more fully described in the first paper of this series (Robinson and van Damme 1966).

* Chatterton Astronomy Department, University of Sydney.

† Division of Radiophysics, CSIRO, University Grounds, Chippendale, N.S.W.

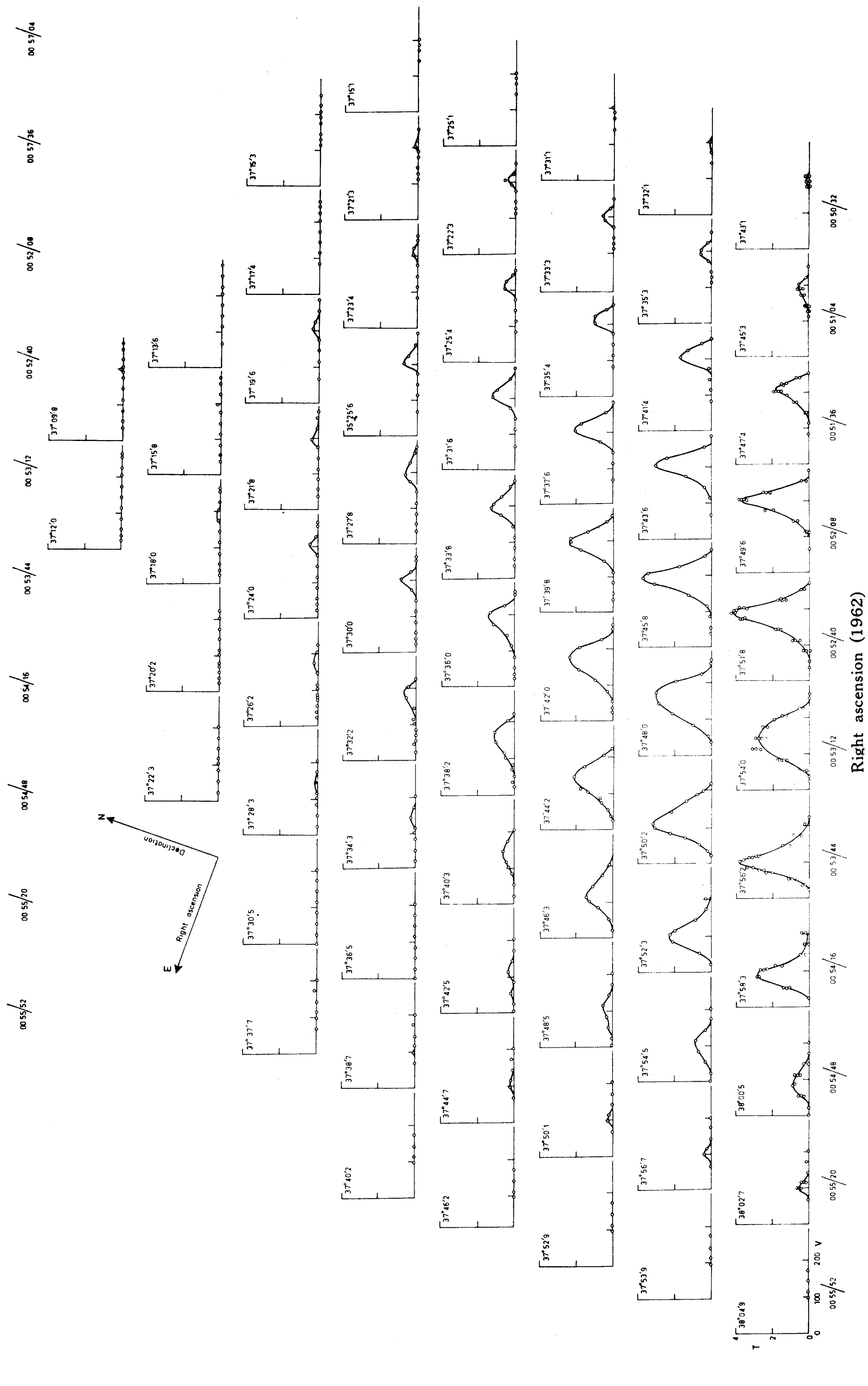

Fig. 1(a).—Grid of HI profiles north of the major axis. The scales of antenna temperature T (°K) and velocity V (km/sec) are marked on the profile at R.A. $00^h\ 55^m\ 52^s$, Dec. $-38°\ 04'{\cdot}9$. All declinations are negative. (The major-axis profiles are shown on both halves of the grid, Figs. 1(a) and 1(b).)

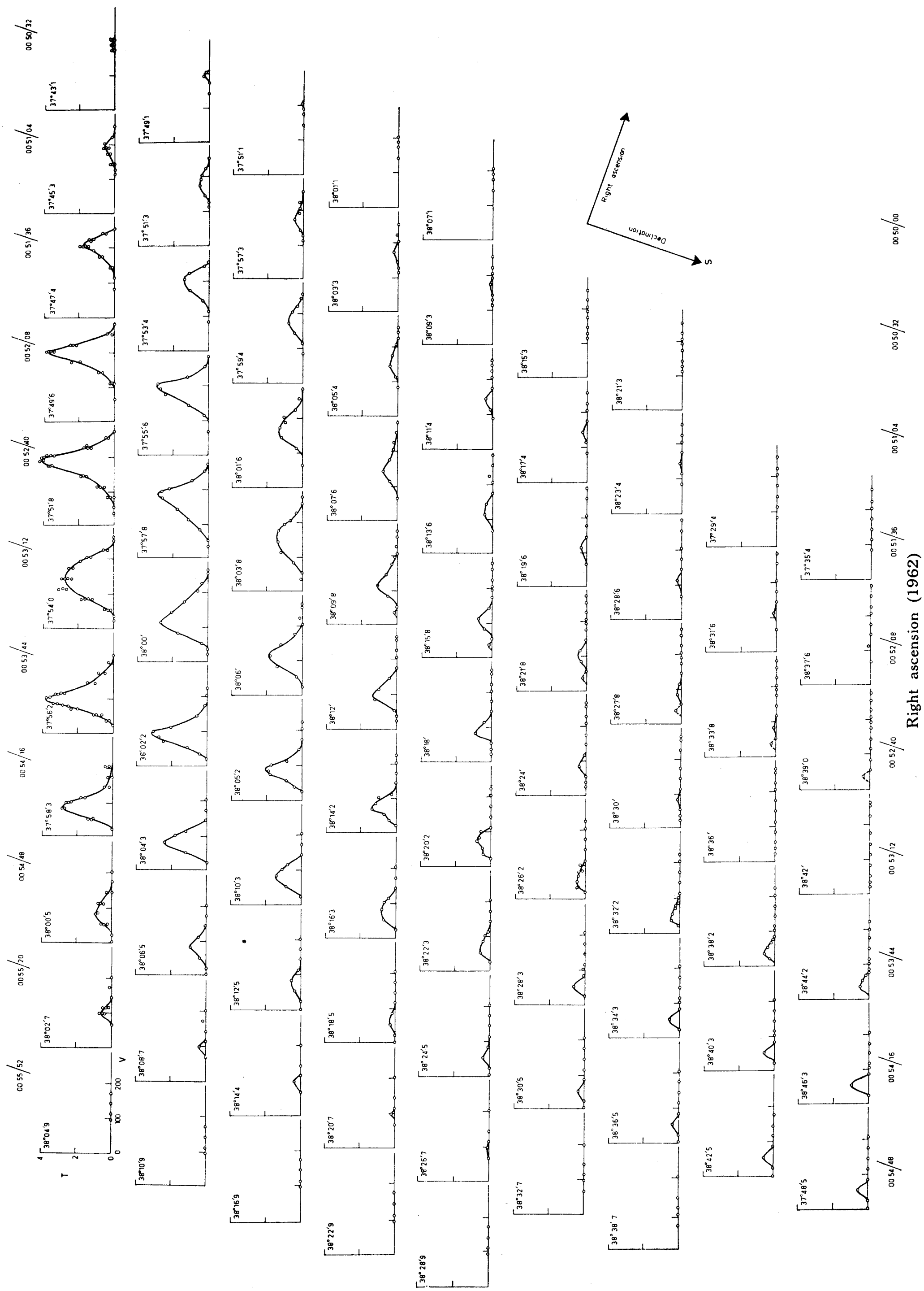

Fig. 1(b).—Grid of HI profiles south of the major axis.

The preliminary observations consisted of scans in right ascension and declination at frequencies corresponding to velocities between about 50 and 250 km/sec, in order to determine the limits of the galaxy. Thereafter, forward and reverse scans in declination were obtained at intervals of 32^s in right ascension and at intervals of 30 km/sec in velocity. From these scans the antenna temperature T_a was obtained at points on the optical major axis and at a series of points spaced 6′ arc north and south of the major axis.

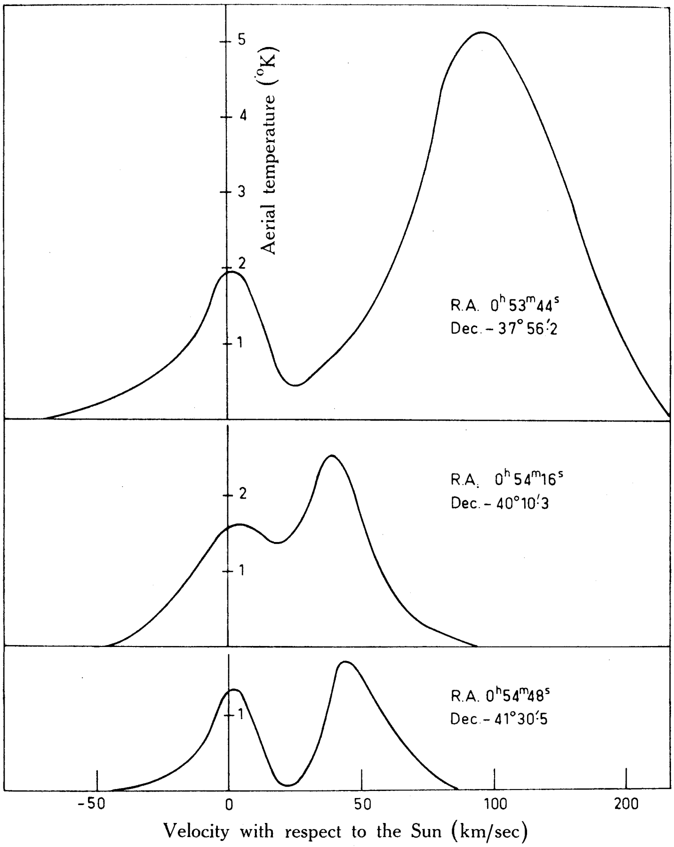

Fig. 2.—Three HI profiles. One profile near the centre of NGC 300 (top) shows also galactic hydrogen at 0 km/sec; the other two show only the "HI cloud" near 40 km/sec plus the galactic hydrogen.

When a sufficient number of these scans had been completed the line profiles for the specific points were constructed. Further scans and point-to-point observations were made in order to define the peaks of some of the profiles with more precision, including some observations at intermediate velocities. The final grid of profiles is shown in Figure 1. The zero points of all the scans were taken at Dec. −36° 54′ (1962·0), 1° north of the galaxy, after it had been verified from right ascension scans at this declination that there was no signal greater than about 0°·1 in this region throughout the range of frequencies used. On the south side of the galaxy the

21 CM OBSERVATIONS OF NGC 300

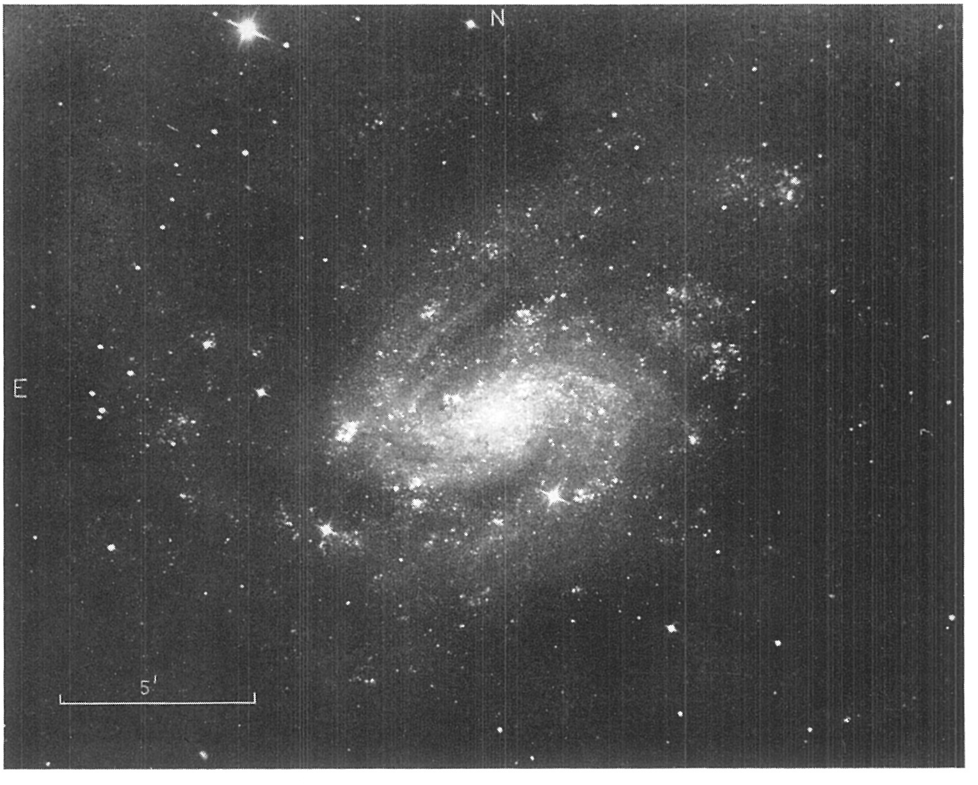

NGC 300 (74 in. Pretoria telescope).

situation is different, since at a velocity of about +40 km/sec aerial temperatures of 0·5–2·5°K were detected at up to 4°·5 from the centre of NGC 300. Some preliminary observations of the area have been made by R. X. McGee using the 48 channel line-receiver (McGee and Murray 1963). Three profiles, one in NGC 300 and two well outside the galaxy, are shown in Figure 2. The first profile shows no obvious signal at 40 km/sec, although the nearby Milky Way gas at zero velocity is evident; the two profiles at about 2° and 3°·5 from the galaxy show zero-velocity gas, and gas at +40 km/sec. The latter appears to extend at least 4°·5 from NGC 300 to the south-east; the east–west extent is probably somewhat less (about 3°).

TABLE 1

OPTICAL PROPERTIES OF NGC 300

Type	SA(s)cd
R.A. (1950)	$0^{h}\,52^{m}\cdot 6$
Dec. (1950)	$-37°\,58'$
Galactic longitude (l^{II})	299°·13
Galactic latitude (b^{II})	−79°·41
Corrected distance modulus (m_0-M)	26·4
Distance (Mpc)	1·9
Total apparent magnitude (m_{pg})	8·66
Integrated luminosity (solar units)	$2\cdot 3\times 10^{9}$
Major-axis position angle (from isophotes)	$109°\pm 3°$
Optical dimensions	30′ by 23′
Linear dimensions (kpc)	16·5 by 12·6
Inclination	$42°\cdot 5\pm 2°$

The observations were taken between May 1963 and April 1964. Further scans of the neighbouring HI cloud were obtained in May 1965. The total observation time was about 200 hours. The great majority of the points marked at each velocity on the profiles (Fig. 1) represent at least two values of T_a. The average number of observations per velocity for the major-axis profiles is three; for the other profiles the value is about two.

III. Optical Characteristics of NGC 300

Isophotes have been constructed by de Vaucouleurs and Page (1962) from Mount Stromlo 74 in. and 30 in. photographs. Plate 1 was taken from the Cape Atlas.

Table 1 gives the position (from the New General Catalogue) and the main optical properties of NGC 300, taken from de Vaucouleurs and Page.

IV. Neutral Hydrogen Content

(a) *Hydrogen Mass*

When the optical depth is small the mass of hydrogen in the galaxy is directly proportional to the integral of the antenna temperature T_a over the sky coordinates and over frequency. In the notation of Robinson and van Damme (1966) the HI mass is

$$M_{\mathrm{H}}/M_{\odot} = 3\cdot 10\, D^2(1-\beta)^{-1}\int\int\int_{\mathrm{c}} T_{\mathrm{a}}(\theta,\phi,\nu)\,\mathrm{d}\theta\,\mathrm{d}\phi\,\mathrm{d}\nu, \qquad (1)$$

where D is the distance in kiloparsecs, β is the beam efficiency, θ, ϕ are the sky coordinates in radians, and ν is the frequency in cycles per second. As in the preceding papers the scale of $T_a/(1-\beta)$ was determined from observations of a source of known flux (3C 353) and the measured solid angle of the beam (207 sq min). For the adopted scale of T_a, $(1-\beta)$ was $0 \cdot 58$.

In order to find the total hydrogen content from the observed HI profiles, three steps were required.

1. Determine the area of each profile, using a planimeter, then for each value of right ascension plot *profile area* against *declination.*
2. Determine the areas of each of these graphs, and plot these areas against *right ascension.*
3. Finally, determine the area under the last graph, and we have the total integrated HI content of the galaxy in units of [km/sec, °K, (min of arc)^2].

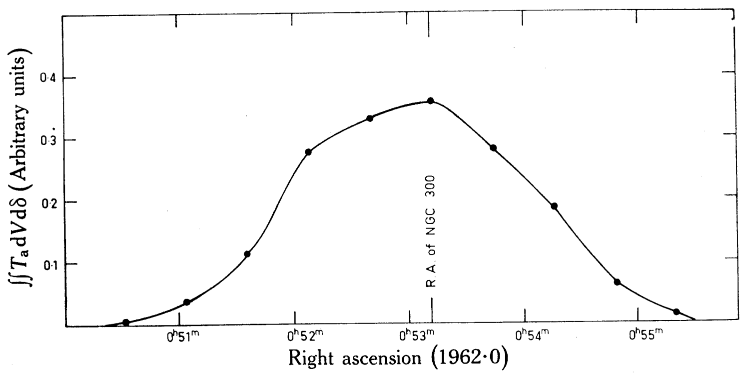

Fig. 3.—HI flux, integrated over declination and velocity, plotted against right ascension to show the east–west asymmetry of the HI content.

The final graph in the above procedure is shown in Figure 3 in order to indicate the quite large difference in HI distribution between the east and west sides of the galaxy. There is 30% more hydrogen to the west of the centre than there is to the east.

Converting the integrated T_a to the units of equation (1), we obtain a mass of HI equal to $2 \cdot 0 \times 10^9 M_\odot$. This does not include the cloud of HI to the south-east of NGC 300. The distance of the galaxy is taken as $1 \cdot 9$ Mpc. Correction for optical depth is small, about 5% when we modify the Epstein (1964*a*) model for an Sc galaxy to allow for the fact that there is only one-quarter as much hydrogen in NGC 300. The corrected mass should thus be $2 \cdot 1 \times 10^9 M_\odot$.

We can estimate the mass of the adjacent HI cloud by assuming its dimensions to be $4° \cdot 5$ by 3°, the mean T_a to be about 1°K, and the mean profile half-width to be 30 km/sec. The mass is then of the order of 10^8–10^9 $M_\odot$, if it is at the distance of NGC 300. This is of the same order of mass as that of dwarf galaxies. If, however, the cloud is only a few kiloparsecs above the plane of our Galaxy, the mass will be only of the order of 10^3 solar masses. Further observations of this cloud are planned with the 48 channel receiver to determine its full extent and whether it shows any rotation. Such rotation would provide valuable evidence as to whether the cloud is extragalactic or not.

(*b*) *Hydrogen Distribution*

The observed line profiles along the major axis have been combined in Figure 4, which shows antenna temperature as a function of observed velocity and distance from the centre. The main HI concentrations lie about half way between the centre and the turnover points of the rotation curve.

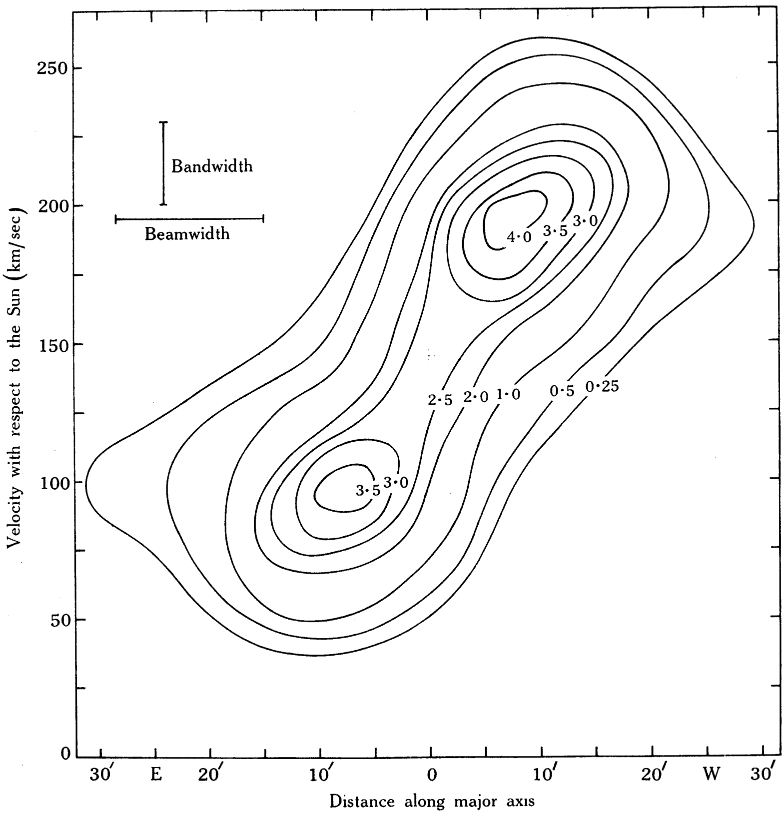

Fig. 4.—Major-axis antenna temperatures shown as a function of observed velocity and distance from the centre of NGC 300.

If we take into account the finite size of the beam it is evident that there is a minimum in the HI distribution around the centre of NGC 300. Similar distributions have been found for M 31 (Burke, Turner, and Tuve 1964; Roberts 1966) and for M 33 (Burke, personal communication). The excess of hydrogen to the west of the centre may also be seen on this figure, which may be compared with Figure 3.

In order to compare the neutral hydrogen distribution with that of the light in the optically visible part of the galaxy, the optical isophotes given by de Vaucouleurs and Page (1962) were convolved with the beam of the 210 ft telescope which, at the half-power points, is $13'\cdot5$ arc (Fig. 5(*b*)). The smoothed isophotes have a ratio of axes of $0\cdot96$, compared with the value for the outer HI isophotes (Fig. 5(*a*)) of $0\cdot73$. We find here that there is about 5% more luminosity to the *east* of the centre than there is to the west. The convolved isophotes may be compared with the HI distribution, where we found 30% more hydrogen to the *west*.

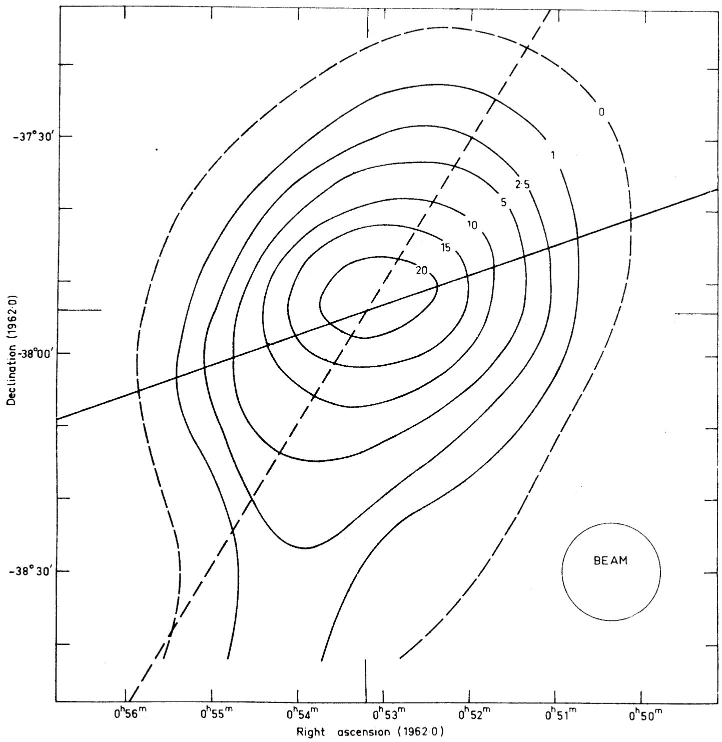

Fig. 5(*a*).—Isophotes showing the distribution of HI over NGC 300 and over the northern part of the neighbouring cloud. To convert contour units to values of $\int_0^\infty T_b(\nu)\, d\nu$, multiply by $1\cdot18\times10^5$ Hz °K. Continuous line is major axis of optical isophotes given by de Vaucouleurs and Page (1962), and of the inner HI isophotes; dashed line is major axis of the outer HI isophotes, with the effect of the neighbouring cloud removed from the south-east side.

The total mass of the galaxy, determined in Section IX, is $2\cdot5\times10^{10}\ M_\odot$. If we assume a constant mass/luminosity ratio across the stellar regions of the galaxy, then the 5% difference in the luminosity corresponds to $6\times10^8\ M_\odot$ difference in mass; that is, there is $6\times10^8\ M_\odot$ more luminous material to the *east* of the centre of NGC 300. The difference in the HI distribution indicates $2\cdot6\times10^8\ M_\odot$ more hydrogen to the *west*, so the combined effect of the asymmetries is that there is $3\cdot4\times10^8\ M_\odot$ more mass to the east of the nucleus, a figure which is uncertain by at least half its value and represents only $1\cdot4$% of the total mass of NGC 300. We then conclude that the centre of mass of the system must be close to the optical nucleus of the galaxy.

The area within which the HI intensity exceeds $0 \cdot 1$°K is 80′ by 60′, with the major axis of the outer isophotes in position angle 149°±3° (Fig. 5(*a*)). The position angle of the inner isophotes is, to within the errors, the same as that of the optical isophotes (109°). This rotation of the major axis may well be a gravitational effect caused by the presence of the nearby HI cloud. The isophotes are clearly distorted

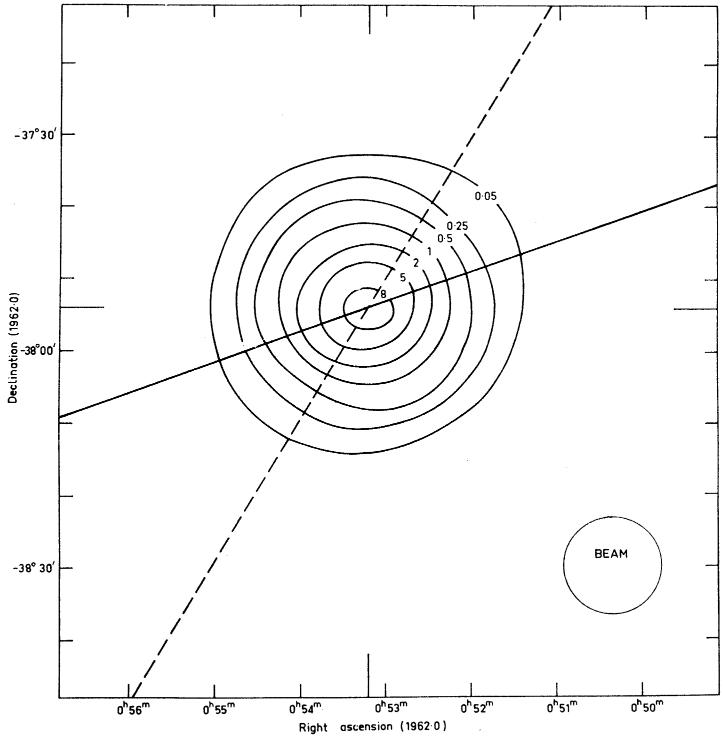

Fig. 5(*b*).—Optical isophotes (blue light) given by de Vaucouleurs and Page (1962), smoothed by the Gaussian beam which is $13' \cdot 5$ diameter at half-power points. The contours are in arbitrary units. Continuous line is major axis of optical isophotes given by de Vaucouleurs and Page, and of the inner HI isophotes; dashed line is major axis of the outer HI isophotes, with the effect of the neighbouring cloud removed from the south-east side.

in the north–west quadrant of the galaxy, which is on the opposite side of the centre of NGC 300 from the cloud. The optical isophotes show no such effect, although they are rather irregular; in any case the main effect in the hydrogen isophotes is not visible until beyond the optical extent of the galaxy.

V. Velocities in NGC 300

(*a*) *Correction of Velocities for Beam Smoothing*

Since the size of the beam of the 210 ft telescope is a significant fraction of the diameter of NGC 300, an attempt was made to correct the major axis HI profiles for the effect of beam smoothing. The method used was similar to that advocated by

Bracewell (1955). At each velocity the mean antenna temperature $\bar{T}_a$ was found for the four profiles surrounding the major-axis profile under consideration. This value is subtracted from the value of T_a for the major-axis profile at this velocity and the result added to T_a to give the "desmoothed" value for T_a. In this way each profile is restored and the new velocities at their peak T_a's determined. The procedure did not change the velocity of the peaks of the three innermost profiles but raised the velocity at the turnover point on the rotation curve by about 5 km/sec (after

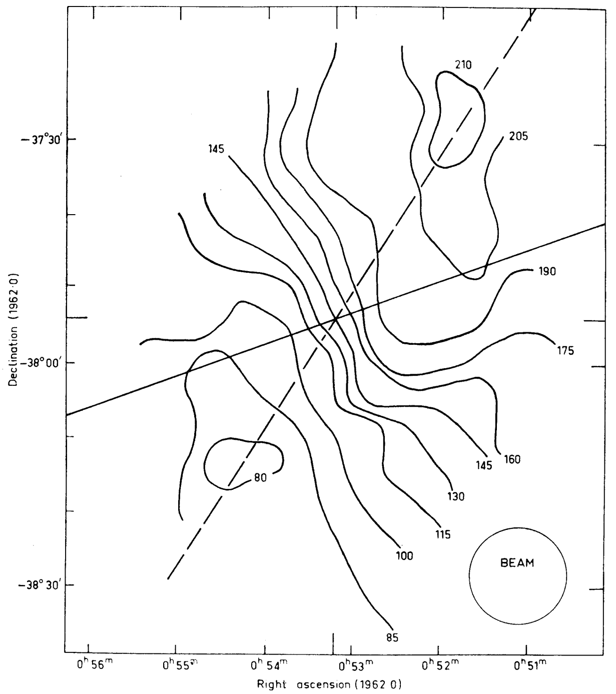

Fig. 6.—Velocity contour map (values in km/sec) for NGC 300. Continuous line is optical major axis; dashed line is axis of outer HI isophotes.

applying the cosec i correction for inclination); the distance from the nucleus at which the turnover point occurs is ill defined, and the restoration procedure did not alter it significantly. The effect of the restoration procedure on the velocity distribution is to raise the mass by 10%.

(b) *The Velocity Contour Map*

In order to find out if the skewness in the neutral hydrogen and in the light distribution, and the presence of the cloud on the south-east side of the galaxy, have any effect on the velocity field in NGC 300, a velocity contour map (Fig. 6) was constructed. It shows several peculiarities.

The "closed" areas on the map, which would normally be found around the turnover points on the rotation curve, are not on the optical major axis. Instead, they lie on an "axis" which passes within 2′ of the centre of the galaxy and which is in position angle $148° \pm 3°$; this, to within the errors, is coincident with the major axis of the outer HI isophotes. However, the axis on which the maximum $\mathrm{d}V/\mathrm{d}r$ occurs, and perpendicular to which we have the straightest velocity contour (that at 145 km/sec, through the nucleus), is the optical major axis in position angle 109°. We note also that if we draw a line from the nucleus normal to the velocity contours, it follows a direction similar to that in which the major axis of the HI contours is

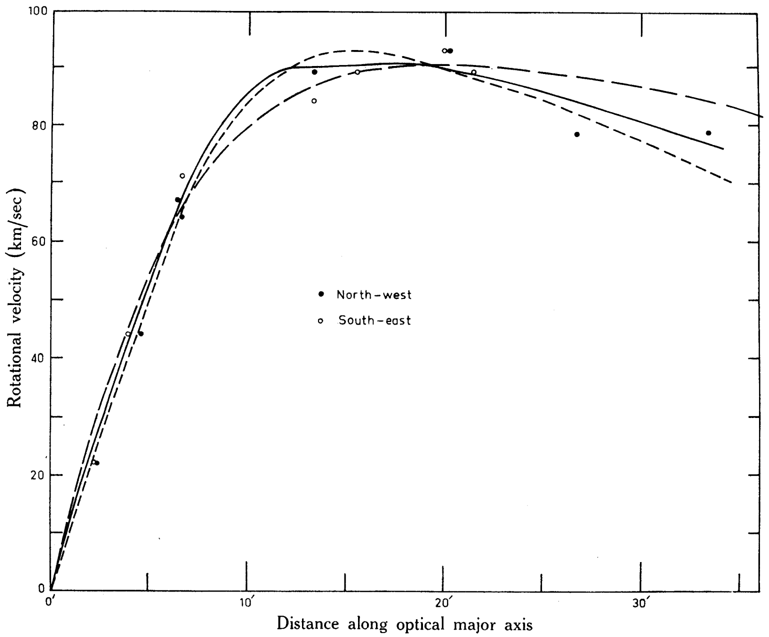

Fig. 7.—Rotation curve of NGC 300 (optical major axis). Velocities are corrected for an inclination of 42°·5 and include the small correction for beam-smoothing. - - - - - Bottlinger–Lohmann function; – – – – Brandt function; ——— Perek two-spheroid model.

rotating. It seems that we have two systems in NGC 300, or at least that the hydrogen in the outer regions is strongly perturbed and is rotating at a higher circular velocity than the gas at the end of the optical major axis. It is probably significant that the peak velocities in the "closed" areas both have the same (observed) velocities with respect to the centre of the galaxy ($210-145 = 145-80 = 65$ km/sec), although they are at different distances from the optical centre. This strongly suggests that the hydrogen off the major axis is rotating in a circular orbit with an axis in position angle 148°.

The systemic velocity of NGC 300 is 145 ± 2 km/sec and is well determined from the central HI profile, from the centre of symmetry of the rotation curve (about the optical major axis), and from the fact that the 145 km/sec contour is the nearest to a straight line on the contour map. This may be compared with the velocity given by Epstein (1964*b*) of 145 ± 10 km/sec and with that in the Humason, Mayall, and Sandage catalogue (1956) of 248 ± 40 km/sec. However, the latter velocity is that of a single HII region near the nucleus, which probably has a large peculiar motion.

VI. Rotation Curve and Mass Estimates

(*a*) *Rotation Curve*

The rotation curve, constructed from the velocities at the peaks of the desmoothed profiles along the optical major axis and from the velocity contour map, is shown in Figure 7. The velocities have been corrected for an inclination of $42° \cdot 5$. The solid circles are from the north-west quadrant, and the open circles from the south-east quadrant. Least-squares fits of the Bottlinger–Lohmann function (short dashes), the Brandt function (long dashes), and a Perek two-spheroid model (continuous line) were made and are discussed below.

(*b*) *Mass from the Kepler Formula*

If we assume spheroidal symmetry for NGC 300, and further that the velocity given by the outermost HI profile refers to a point just outside the galaxy, then we may use the formula $M = rV_r^2/G$, where r and V_r are the distance and velocity, respectively, of this point.

The outermost HI profile along the optical major axis shows a peak rotational velocity (corrected for an inclination of $42° \cdot 5$) of 79 km/sec, at a distance of $33' \cdot 4$ from the nucleus. If we assume that the distance of NGC 300 is $1 \cdot 9$ Mpc, then the mass using the Kepler formula becomes $2 \cdot 6 \times 10^{10}\ M_{\odot}$, where $M_{\odot}$ is the mass of the Sun. This velocity, however, may be in error by up to 10 km/sec, so that the error in the mass is $0 \cdot 7 \times 10^{10}\ M_{\odot}$.

We must note here that the maximum velocities, and the maximum HI extent of the galaxy, are observed along the position angle 148°. The outermost observed velocity in this direction is 60 km/sec, occurring at a distance of 42′ from the nucleus of NGC 300. Using this velocity the minimum mass given by the Kepler formula is $1 \cdot 93 \times 10^{10}\ M_{\odot}$, but if we assume an inclination of $42° \cdot 5$ the mass becomes $4 \cdot 2 \times 10^{10}\ M_{\odot}$. Further discussion on the inclination and thickness of NGC 300 is given in Section VII.

(*c*) *Mass from the Bottlinger–Lohmann Function*

A fit of the Bottlinger–Lohmann function (Lohmann 1954) to the observed rotation curve was made using a least-squares procedure. A total of 15 velocities was used, from the major-axis HI profile peaks and from the velocities on the velocity contour map where the contours cross the major axis. This function is shown in Figure 7. The fit is not very good; the function places the turnover point at about 15′ arc from the nucleus, whereas the maximum velocities are observed to occur at about 22′ arc. However, the mass given by the Bottlinger–Lohmann function is $2 \cdot 5 \times 10^{10}\ M_{\odot}$, close to that obtained from the Kepler formula.

(d) *Mass from the Brandt Function*

The function given by Brandt (1960) does not fit the observed rotation curve. The mass derived from the curve of best fit is twice that from the Bottlinger–Lohmann function.

(e) *Mass using a Pair of Oblate Spheroids*

Perek (1950) has proposed that a model of a galaxy may be constructed in the form of a nonhomogeneous oblate spheroid. However, it was found for NGC 55 (Robinson and van Damme 1966) and for NGC 300 that the rotation curve for a single spheroid falls off much too steeply after the turnover point. Consequently, we have combined two spheroids, which we will call the "inner" and "outer" spheroids; the relationships between them are:

	Radius	Axis Ratio	Central Density
Inner spheroid	$0\cdot5a$	$0\cdot2$	ρ_c
Outer spheroid	a	$0\cdot4$	$\frac{1}{6}\,\rho_c$

Density law: $\rho = \rho_c(1-m^2)^2$, where $m^2 = (x^2+y^2)/a^2+z^2/c^2$;

a is the radius of the galaxy along the optical major axis, which is taken as $5\cdot09\times10^{22}$ cm (equivalent to 30′ at $1\cdot9$ Mpc).

When the rotation curve computed from this model is normalized to fit the observed velocities (continuous line in Fig. 7) we find that $\rho_c = 3\cdot26\times10^{-24}$ g/cm^3. Thus, the central density (averaged over the beam) of NGC 300, which is $\frac{7}{6}\,\rho_c$, becomes $3\cdot80\times10^{-24}$ g/cm^3. The mass of the inner spheroid is $0\cdot52\times10^{10}\,M_\odot$ and of the outer spheroid is $1\cdot44\times10^{10}\,M_\odot$. The total mass of the galaxy is thus $2\cdot0\times10^{10}\,M_\odot$. This is most likely to be an underestimate, since the density on this model is zero at the point where the hydrogen falls below the detection limit of the 210 ft telescope. It is possible that there is some material outside this limit. In fact, we do observe hydrogen associated with the galaxy extending to beyond 40′ in the north-west and south-east directions (*not* including the cloud), and if this has not significantly altered the rotation along the optical major axis it will not be included in the mass of the model.

VII. Rotation Curve and Total Mass from the Major Axis of the HI Distribution

The maximum velocities in NGC 300 and the maximum extent of the neutral hydrogen distribution are found along the line in position angle 148°. This suggests that perhaps the hydrogen is aligned with this axis, or that there is a concentration of hydrogen in the north-west and south-east quadrants of the galaxy. If we fit the velocity curve of the Perek two-spheroid model to the "rotation curve" along this axis we find a mass twice as large as that derived from the optical major-axis rotation curve (using $i = 42°\cdot5$). As we mentioned in Section VI, the minimum mass given by the Kepler formula (with $i = 0°$) is $1\cdot93\times10^{10}\,M_\odot$. If the inclination is $42°\cdot5$ the mass is increased to $4\cdot2\times10^{10}\,M_\odot$. However, the ratio of minor to major axes of the outer HI isophotes is $0\cdot73$, and if we assume the ratio of thickness to diameter is $0\cdot2$ then $i = 32°$ and the Kepler mass is $6\cdot9\times10^{10}\,M_\odot$. These latter values are evidently too high and in fact give a mass/luminosity ratio of 20–30, which is much higher than that for other Sc galaxies. We conclude that either the large cloud of HI to the south-east of NGC 300 is dynamically affecting the galaxy or there are two large condensations of hydrogen to the north-west and south-east which have produced an apparent rotation of the major axis of the HI distribution.

VIII. Mass Distribution

Since the two-spheroid model (Section VI(a)) fits the observations best, we show in Figure 8 the density distribution (projected onto the plane of the galaxy) for inner and outer spheroids and for the combined model. The ordinate is in units of $(1-m^2)^2$, and $1\cdot 0$ corresponds to $\rho_c = 3\cdot 26\times 10^{-24}$ g/cm^3, the central density of

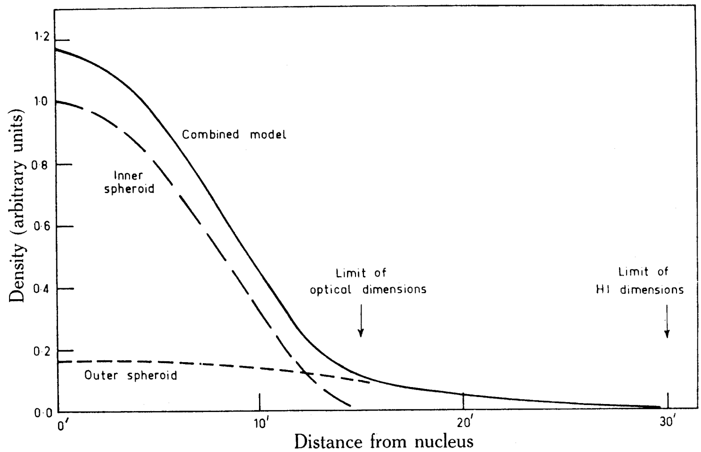

Fig. 8.—Density distribution for the two Perek spheroids separately and for the combined model.

the inner spheroid. This distribution is obviously affected by the size of the beam of the 210 ft telescope, and the central density will be appreciably higher than the $3\cdot 8\times 10^{-24}$ g/cm^3 given by the model. However, the nucleus of NGC 300 is not very prominent, and a value of about 2×10^{-24} g/cm^3 will be a good estimate for the mean projected density of the optical part of the galaxy, at least.

IX. Summary of Mass Estimates for NGC 300

The best fit to the observed velocities is evidently that of the Perek two-spheroid model, which gives a mass of $2\cdot 0\times 10^{10}\ M_\odot$. However, as we have observed, this is probably a minimum value of the mass. Both the Kepler formula and the Bottlinger–Lohmann function (for the optical major axis) give a higher mass, with larger uncertainties, and the minimum value for the Kepler mass obtained from the outermost velocity in the north-west quadrant is $1\cdot 93\times 10^{10}\ M_\odot$. So we shall take for the mass of NGC 300 the value of $2\cdot 5(\pm 0\cdot 5)\times 10^{10}\ M_\odot$.

The luminosity of NGC 300 is $2 \cdot 3 \times 10^9\ L_\odot$ (de Vaucouleurs and Page 1962), and the HI mass is $2 \cdot 1 \times 10^9\ M_\odot$ (from Section IV), so that we have for NGC 300 the following ratios:

$$M_{\mathrm{HI}}/M_{\mathrm{T}} = 0 \cdot 084; \qquad M_{\mathrm{T}}/L = 10 \cdot 9; \qquad M_{\mathrm{HI}}/L = 0 \cdot 91.$$

These values are very close to those derived by de Vaucouleurs and Page from their own and Epstein's data (0·095, 9·0, and 0·86 respectively).

X. References

Bracewell, R. N. (1955).—*Aust. J. Phys.* **8**, 54.

Brandt, J. C. (1960).—*Astrophys. J.* **131**, 293.

Burke, B. F., Turner, K. C., and Tuve, M. A. (1964).—Symp. IAU–URSI No. 20 (Canberra 1963). p. 99.

Epstein, E. E. (1964*a*).—*Astr. J.* **69**, 521.

Epstein, E. E. (1964*b*).—*Astr. J.* **69**, 490.

Humason, M. L., Mayall, N. U., and Sandage, A. R. (1956).—*Astr. J.* **61**, 97.

Lohmann, L. (1954).—*Z. Astrophys.* **35**, 159.

McGee, R. X., and Murray, J. D. (1963).—*Proc. Instn Radio Engrs Aust.* **24**, 191.

Perek, L. (1950).—*Bull. astr. Insts Csl.* **2**(5), 75.

Roberts, M. S. (1966).—*Astrophys. J.* **144**, 639.

Robinson, B. J., and van Damme, K. J. (1966).—*Aust. J. Phys.* **19**, 111.

de Vaucouleurs, G., and Page, J. (1962).—*Astrophys. J.* **136**, 107.